Management and Production Engineering Review
Volume 15 • Number 1 • March 2024 • pp. 100–110
DOI: 10.24425/mper.2024.149993

Integrating a Complete Approach for Optimization and Sustainability in Brake Disc Rotors

Hicham Fihri FASSI, Reda OURIHI, Fatima Zohra EL HILALI

Hassan First University of Settat, Faculty of Sciences and Techniques, LIMII, Team Ecoesign Energy & Innovation, Settat, Morocco

Received: 17 September 2023
Accepted: 16 December 2023

Abstract
This study employed two primary approaches to determine the optimum structure: the lightweight and sustainable models. The lightweight model considered various factors such as materials, geometry, and dimensions of the brake disc rotor and brake pads. On the other hand, the sustainable model considers the manufacturing process and aims to reduce the carbon footprint. To calculate the optimal lightweight structure, finite element analysis was conducted using two different materials to compare the resulting stresses and determine the most appropriate material. Subsequently, four different models were utilized in finite element analysis to evaluate the displacement and stress and establish the optimum structure. Regarding sustainability, two distinct processes were employed to assess the environmental impact and energy consumption to adopt an eco-friendly approach. This paper investigates the transition from the initial brake disc rotor to a lightweight model, employing finite element analysis, topology optimization, and sustainability considerations. The work is achieved by comparing the cost between conventional and 3D printing processes.

Keywords
3D printing, Additive Manufacturing, Topology Optimization, FEA, Sustainability, Brake Disc Rotor.

Introduction

For numerous years, computer simulators have enabled the demonstration of the operational principles of disc brake rotors, the pressure exerted by brake fluid, the distribution of this pressure across various circuits, and the forces acting upon each component. These simulations have contributed to a deeper understanding of such systems. Furthermore, when the brake system is engaged, it becomes crucial to subject the involved variables and the vehicle's behavior to different scenarios (Talati & Jalalifar, 2008; Gumiel et al., 2024; Veeman et al.,, 2024). Presently, incorporating simulation elements alongside engineering tools is imperative to streamline the work of engineers, providing them with a precise framework for approaching vehicle systems efficiently, safely, and technically. An integrated approach can be developed through data collection and physical measurements, enabling the brake system's dimensioning, analysis, and modification (Yan et al., 2022; Wei et al., 2024; Isacco et al., 2024).

The primary aim of this study is to establish a methodology for designing brake system parameters using a lightweight and sustainable model. The significance of this approach lies in its ability to expedite the analysis of brake system dimensions, facilitating efficient implementation and necessary modifications to enhance system performance. It is worth highlighting that this research will adopt an analytical method, utilizing real data and formulas to conduct various calculations of the vehicle's brake system. Practical measurements will be employed to validate the proposed approach and corroborate the accuracy of the results (Elhilali et al., 2024; Deng et al., 2024; Sahoo et al., 2024).

Mathematical analysis

The brake system is a critical mechanism in a vehicle that converts the vehicle's motion into heat through energy absorption. Its primary function is to ensure the driver's and passengers' safety by effectively stop-

***Corresponding author**: Hicham Fihri Fassi – Faculty of Sciences and Techniques, Hassan First University of Settat, Morocco, e-mail: hichame.fihri-fassi@uhp.ac.ma*

ping the vehicle's wheels. Over the past decade, significant advancements have been made in studying heat dissipation and determining materials for brake discs, considering their intended purpose (Hamada & Orhan, 2022; Kumbhar et al., 2017; Ma et al., 2024). Therefore, it is essential to consider the specific usage conditions to appropriately choose reliable components that prevent system overheating and potential failures.

Braking Force

The braking force application to a moving vehicle, which possesses kinetic energy, can be equated to the driving force resulting from the average displacement speed. This braking effect involves converting the vehicle's kinetic energy into heat, which occurs through friction between the mechanical components of the brakes (Kamiński, 2022; Rahmzadeh et al., 2024; Garg et al., 2024). The primary role of the brake caliper is to convert hydraulic pressure transmitted through ducts or the pulling force exerted by a brake cable into a linear mechanical force. N.P. Wagh (Wagh, 2005; Kladovasilakis et al., 2024; Huchtkoetter et al., 2024) provides a calculation method for determining the linear forces generated within brake calipers:

$$F_a = P \times A \tag{1}$$

$$F_r = F_a \times \mu \tag{2}$$

With:

F_r: Frictional force

F_a: Applied force generated in the brake calliper

P: Pressure

A: Pad area

μ: Friction coefficient

In Figure 1, the cylinder exerts Pressure denoted as P_a on the brake pad, and in turn, the Brake Pad applies a frictional force denoted as F_a on the Disc Rotor.

Braking Torque

The braking torque is generated through the friction between the brake pads and the disc rotor, resulting in a frictional force that produces the braking torque. To determine the braking force at work, it is assumed that the pressure is uniform, and the braking torque provided by the brake system should be equivalent to the moment the friction forces act relative to the center of the wheel. Therefore, calculating this moment is sufficient to determine the braking torque the brakes need to generate (Wang et al., 2024, Singh & Sarkar, 2024; Mrausi et al., 2024).

$$T = F_r \times R \tag{3}$$

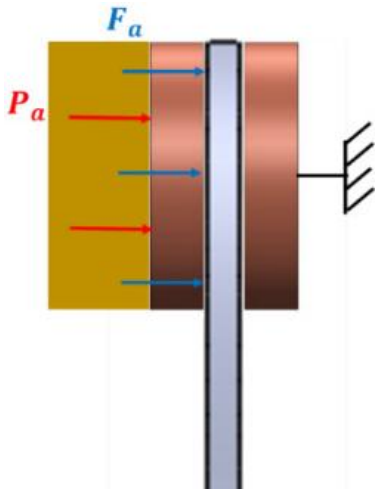

Fig. 1. The function of braking pads

The variables are defined as follows:

T: Brake torque

F_r: Frictional force

R: Radial distance on brake pad from the disc center

The torque capacity of disc brakes can be calculated using two different theories or approaches:

Uniform pressure theory

- Pressure is uniformly distributed over the rubbing surface or the friction Pads.
- Valid for new brake Pads.
- Not valid for old brake pads.

With

$$P = P_a = \text{constant} \tag{4}$$

P_a: Maximum applied Pressure.

By the braking force theory, as expressed in Equations 1 and 2, and the uniform pressure theory, as indicated in Equation 4, the following relationships hold (Fig. 2):

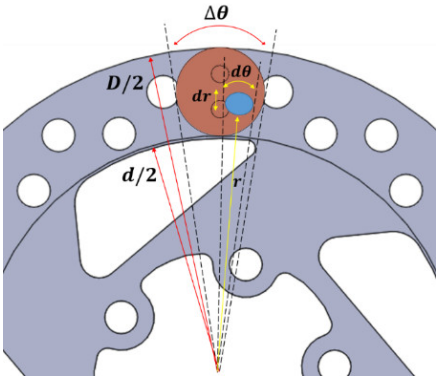

$$F_r = P_a \times A \times \mu \tag{5}$$

Fig. 2. The position of the brake pad and brake disc

In Figure 2, we can observe the following:

$$dA = r \times dr \times d\theta \tag{6}$$

$$A = \int_{-\Delta\theta/2}^{\Delta\theta/2} \int_{d/2}^{D/2} r \times dr \times d\theta \tag{7}$$

$$A = \frac{\Delta\theta(D^2 - d^2)}{8} \tag{8}$$

$$F_r = P_a \times \frac{\Delta\theta(D^2 - d^2)}{8} \times \mu \tag{9}$$

Based on the braking torque theory, as represented by Equation 3, and the relationship derived from Equation 9, we can deduce the following:

$$T = P_a \times \frac{\Delta\theta(D^2 - d^2)}{8} \times \mu \times R \tag{10}$$

For a disc brake system with two friction pads, the following characteristics can be observed:

$$T = P_a \times \frac{\Delta\theta(D^2 - d^2)}{4} \times \mu \times R \tag{11}$$

Uniform wear theory

$$P \times V = P_a \times r \times \omega = \text{constant} \tag{12}$$

- Wear is uniformly distributed over the rubbing surface or friction pads
- Valid for old brake pads
- Wear different radii of friction pads

The variables are defined as follows:
P: Pressure intensity
V: Rubbing velocity
r: Radial distance on brake pad from disc centre
ω: Angular velocity = constant

$$P \times r = \text{constant} \tag{13}$$

Material and Methods

The methods utilized in this study are categorized into three parts. The first simulation employs a mathematical model for static finite element analysis to investigate displacement, stress, and strain. Two different materials, Cast Alloy Steel for model 1 and All 1060 Alloy for model 2, are considered in this analysis. Moving on to the second simulation, after identifying the suitable material, topology optimization analysis is performed on four distinct models: models 1 & 2 with four holes, model 3 with five holes, model 4 with six holes, and model 5 with seven holes (Fihri-Fassi et al., 2024; Cheng et al., 2024; Yu et al., 2024). In the third simulation, following the selection of the optimal structure, the focus shifts towards examining environmental aspects such as air acidification, water eutrophication, carbon footprint, and energy consumption. Two different manufacturing processes, Sand Casted and Milled, are evaluated in this context (Ourihi et al., 2024; Meiklejohn et al., 2024, Adeyi et al., 2024).

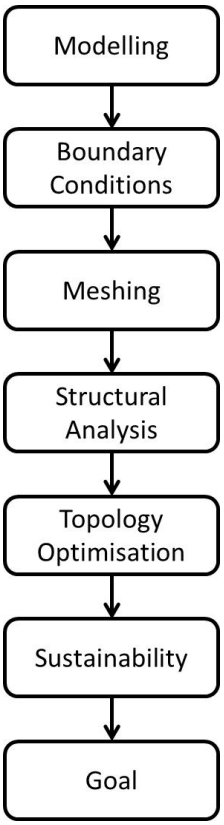

Fig. 3. Flowchart of the process

The theoretical method relies on calculating the independent variables provided by the user and inputting them into a mathematical model. This process allows for the determination of key dependent variables, such as the diameter of the brake discs, the force generated in the brake caliper, and the braking torque. To execute the simulation in SolidWorks, the parameters of the theoretical method must be defined.

The materials utilized for the execution of this project are based on the general data obtained from the brake system of the "Xiaomi Pro 2 scooter" (Figure 4). These data encompass various aspects including measurements, weight, and material properties of the brake pads and brake disc rotor. The specific details of these materials can be found in Table 1 and Table 2.

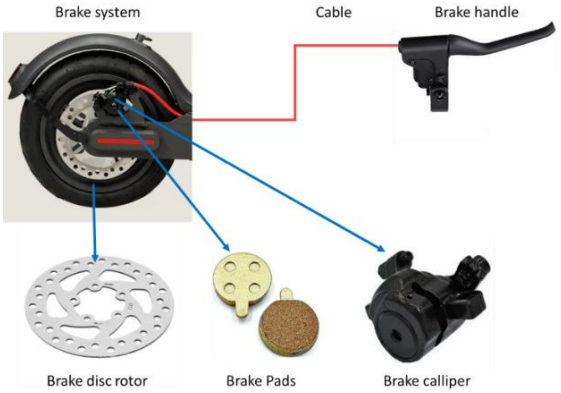

Fig. 4. Braking system components (Made in China, 2024)

Table 1
The Material Properties of Brake Pads (Made in China, 2024)

Property	Carbon Ceramic	Units
Thermal Conductivity	8	W/m°C
Density	1600	kg/m^3
Elastic Modulus	7 E+10	Pa
Specific Heat	1.123	J/kg°C
Ultimate Compressive Strength	1.9 E+8	Pa
Maximum Temperature Use	1750	°C
Poisson's Ration	0.1	

Table 2
Material Properties of Brake disc rotor (Singh, R.K., & Sarkar, C. (2024)

Property	Cast Alloy Steel	All 1060 Alloy	Units
Elastic Modulus	1.9 E+11	6.9 E+10	N/m^2
The Ratio Poisson	0.260	0.33	
Shear Modulus	7.80 E+10	2.7 E+10	N/m^2
Mass Density	7300	2700	kg/m^3
Tensile Strength	4.48 E+08	6.89 E+07	N/m^2
Yield Strength	2.41 E+08	2.75 E+07	N/m^2
Thermal Expansion Coefficient	1.5 E–05	2.4 E–05	/K
Thermal Conductivity	38	200	W/(m·K)
Specific Heat	440	900	J/(kg·K)

Modeling of Disc Brake Rotor

The objective of this calculation is as follows:

- To establish the geometry of the Brake Disc and Pad.
- To apply appropriate meshing techniques for the simulation.
- To determine the necessary boundary conditions, including the braking force, braking torque, and pressure.
- To evaluate the results obtained from running the simulation using SolidWorks.

Geometry

To design the brake disc rotor and brake pads, SolidWorks was employed, as previously stated. The dimensions of the components were obtained manually by measuring the old vehicle's parts. Additionally, other essential specifications were sourced from the vehicle catalogue to ensure accurate design and compatibility.

The brake disc rotor (Figure 5) is affixed at five hub-mounting points and rotates along with the wheel. When the driver applies the brakes, the brake caliper is actuated and exerts pressure on the brake pads (see Figure 6). Consequently, the brake pads generate a frictional force that is applied to the disc rotor.

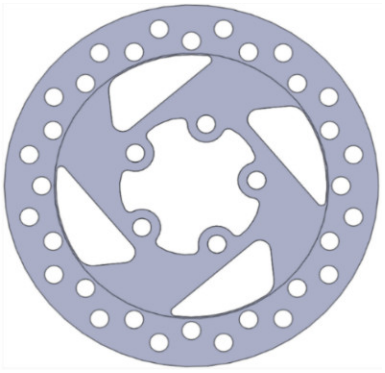

Fig. 5. Brake disc rotor

Fig. 6. Brake disc pad

Boundary Conditions

During the experimental test conducted using an old brake pad, the vehicle could come to a complete stop within 6.5 meters. This test was performed under extreme conditions of hard braking, where the initial velocity of the vehicle was 32 km/h, and it came to a halt at 0 km/h.

It should be noted that Equation 10 for calculating the braking torque is applicable only for new brake

Table 3
Braking system dimensions and vehicle specifications

Property	Abbreviation	Value	Units
Brake disc outer diameter	D	120	mm
Brake disc inner diameter	d	88	mm
Brake disc thickness	E	2	mm
Clamp holes number	n	36	
Thickness of pad	e	4	mm
Pad area	A	201	mm^2
Speed of the vehicle	V	32	km/h
Weight of the vehicle	M_1	14.2	kg
Weight of the user	M_2	72	kg
Stopping distance	s	6.5	m
Brake Disc Weight	M	106	g

pads. The uniform wear theory is utilized for old brake pads, which necessitates knowledge of the pressure P. In such cases, the braking torque can be calculated using Newton's law of motion (Bhat et al., 2024; Mahfouz et al., 2024; Usmani et al., 2024).

Based on the motion equation, which describes the relationship between force, mass, and acceleration, the following principles apply:

$$v^2 = u^2 + 2as \tag{14}$$

The variables are defined as follows:
u: Starting (initial) velocity
v: Final velocity
a: Acceleration
s: Distance
As a result, the following can be deduced:

$$a = 6.078 \text{ m/s}^2 \tag{15}$$

During hard braking in a two-wheeler, approximately 70% of the weight of the vehicle is transferred to the front end. This ratio corresponds to the coefficient of friction (μ) between the brake pads and the disc rotor.

Referring to Table 3, we can extract the relevant information as follows:

$$F_r = \mu \times (M_1 + M_2) \times a \tag{16}$$
$$F_r = 366.739 \text{ N} \tag{17}$$

According to Equation 3

$$T = 22.004 \text{ N} \cdot \text{m} \tag{18}$$

According to Equation 2

$$P_a = 26.065 \text{ bar} \tag{19}$$

Meshing

In Finite Element Analysis, the convergence of the numerical solution depends on the type of meshing employed (Nguyen et al., 2024; Kumar et al., 2024; Kien & Zhuang, 2024). Finer meshing leads to more accurate results. In this article, a finer meshing approach was adopted by utilizing a triangulated surface mesh with a tolerance of 0.07 mm and an element size of 1.5 mm for both models, as depicted in Figure 7. Consequently, the brake disc rotor was divided into 37,374 elements and 66,690 nodes, as indicated in Table 4.

Table 4
Mesh Details and Optimisation Parameters

Property	Value	Units
Mesh type	Solid Mesh	
Jacobian points	16 points	
Element size	1.5	mm
Tolerance	0.07	mm
Total nodes	66690	
Total elements	37374	
Maximum Aspect Ration	11.851	
Optimisation Type	Topology	
Maximum Design Response Values	Strain Energy	
Constraints	Volume	
Fraction of the initial value	0.3	
Geometry Constraint	Frozen Area and Demold Control	

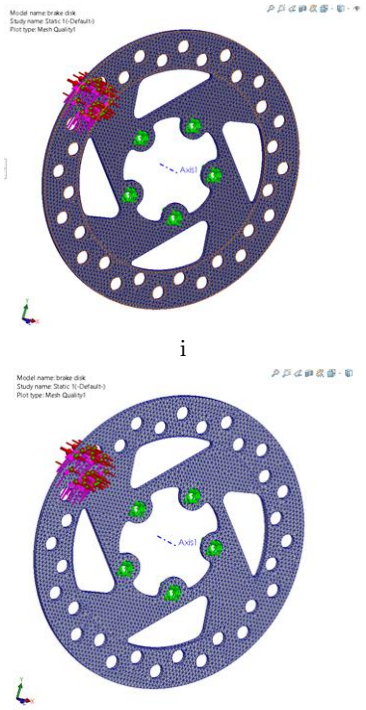

Fig. 7. Model 1 and 2 – Mesh using Cast Alloy Steel for (i) Mesh using All 1060 Alloy for (ii)

Structural Analysis

In the structural analysis, a brake pad pressure (P_a) was applied to both brake disc pads, while a brake torque (T) was applied to the brake disc rotor around its axis of rotation. The results obtained from the finite element analysis revealed that the displacement of model 1 accounted for 35.87% of the displacement of model 2, as indicated in Table 5. Moreover, it was observed that the maximum stress encountered when using the Cast Alloy Steel (CAS) material remained below the yield strength, whereas the maximum stress recorded with the All 1060 Alloy material exceeded the yield strength, as outlined in Table 2 ((Tomozei et al., 2024; Makeshkumar et al., 2024).

Table 5
Results of the simulations for model 1 and 2

Property	Cast Alloy Steel	All 1060 Alloy	Units
Static Displacement	1.445 E–02	4.028 E–02	mm
Static Stress	8.595 E+07	8.417 E+07	N/m^2
Static Strain	3.800 E–04	1.082 E–03	

Topology Optimisation

Based on the previous results presented in Figure 8 and 9, Cast Alloy Steel (CAS) has been selected as the validated material for the brake disc rotor. In the subsequent simulations, the number of larger holes was increased from four to five for model 3, six for model 4, and seven for model 5. The outcomes demonstrated that with an increasing number of holes, the displacement, stress, and strain also increased progressively, as outlined in Table 6. Furthermore, it should be noted that the maximum stress in model 5 remained below the yield strength by a margin of 0,226 E+08 N/m^2.

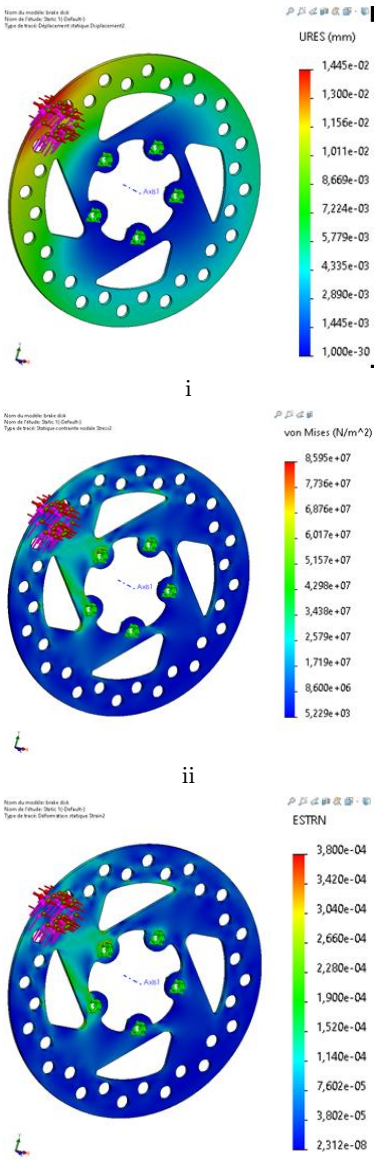

Fig. 8. Showcases the following aspects for Model 1: (i) Static Displacement (ii) Static Stress for (iii) Static Strain

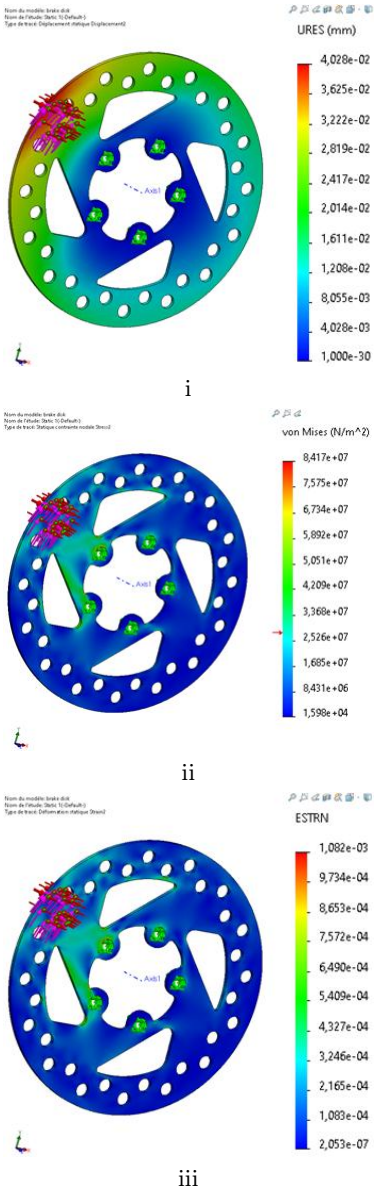

Fig. 9. Showcases the following aspects for Model 2: (i) Static Displacement (ii) Static Stress for (iii) Static Strain

Table 6
Results of the simulations for Model 1, 3, 4 and 5

Property	Model 1	Model 3	Model 4	Model 5	Units
Static Displacement	1.445 E–02	1.872 E–02	2.531 E–02	4.120 E–02	mm
Static Stress	8.595 E+07	1.042 E+08	1.327 E+08	2.184 E+08	N/m^2
Static Strain	3.800 E–04	4.606 E–04	5.865 E–04	9.658 E–04	

Sustainability

Based on the comprehensive analysis of the previous results depicted in Figures 10, 11, and 12, it has been determined that Model 5 stands out as the optimal structure. This selection has resulted in a remarkable weight reduction of approximately 17.5%, significantly decreasing the original weight from 106 g to 87.41 g. This substantial reduction also contributes to material savings and potential cost reductions. Furthermore, an in-depth assessment of the environmental impact associated with the optimum structure was conducted using the eco-design platform developed by Professor H. FIHRI FASSI (Fihri-Fassi et al., 2024), which relies

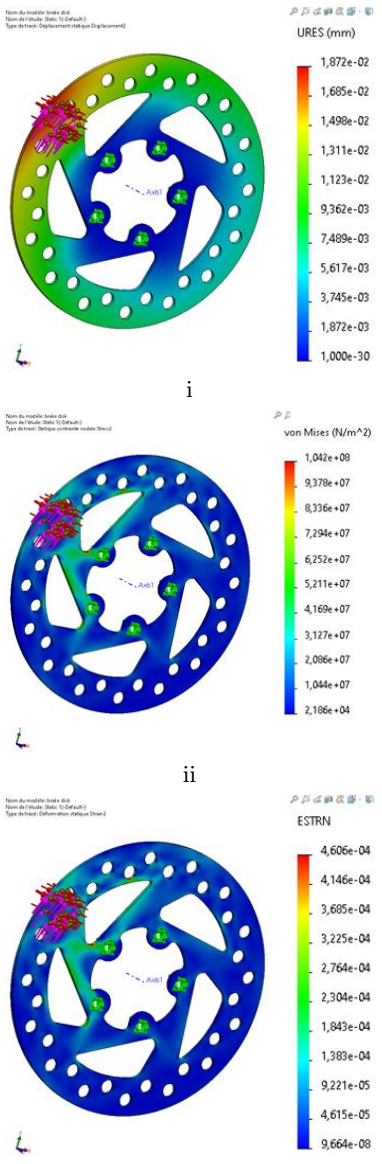

Fig. 10. Showcases the following aspects for Model 3: (i) Static Displacement (ii) Static Stress for (iii) Static Strain

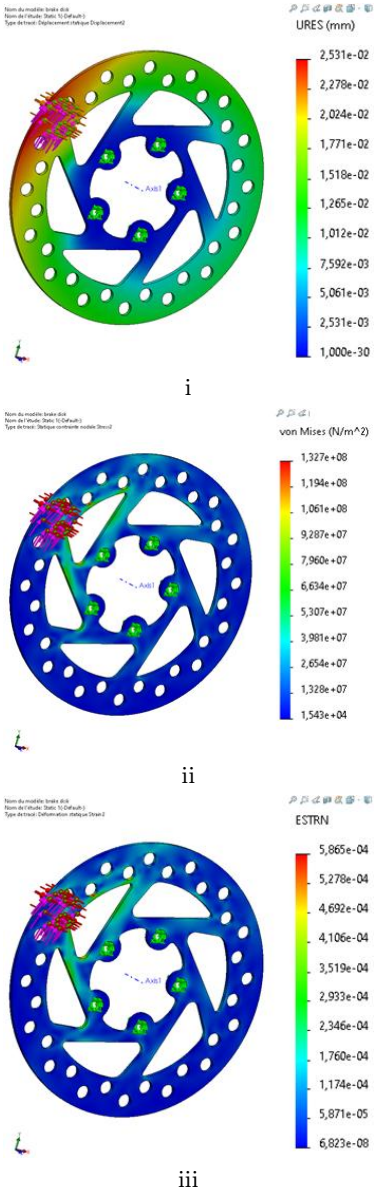

Fig. 11. Model 4 – Static Displacement for (i) Static Stress for (ii) Static Strain for (iii)

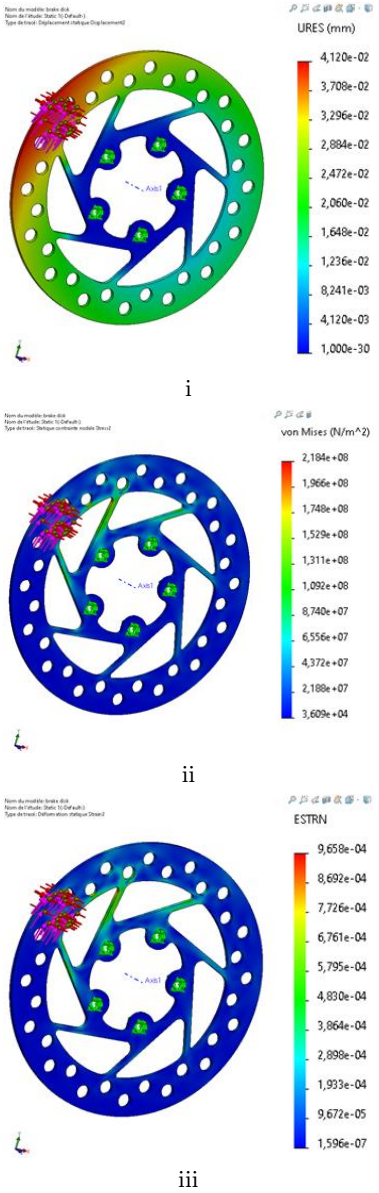

Fig. 12. Model 5 – Static Displacement for (i) Static Stress for (ii) Static Strain for (iii)

on the FD E1-008 database. The evaluation focused on various environmental parameters, including the emission of polluting gases such as CO_2, SO_2, and PO_4.

The results of the assessment demonstrated that the Milled process, employed in the production of the optimum structure, exhibited significant advantages in terms of environmental impact. It emitted considerably lower quantities of polluting gases compared to the Sand Casted process, as presented in Table 7. This finding underlines the environmentally friendly nature of the Milled process and its potential to contribute to sustainable manufacturing practices. Taken together, the weight reduction achieved through Model 5's design optimization, coupled with the environmentally favorable attributes of the Milled process, reinforces the significance of adopting an integrated approach that prioritizes both optimization and sustainability in brake disc rotor manufacturing.

Taking into account the cost aspect (Table 8), the comparison between the printing process and the milled process reveals a notable difference. The printing process offers a cost advantage of $23.12, presenting a more affordable option. On the other hand, the milled process incurs a higher expense of $86.13. This considerable cost disparity indicates that choosing the printing process could be a more economically viable

Table 7
The environmental impact of Sand Casted and Milled processes

	Property	Sand Casted	Milled	Units
General information	Material	Cast Alloy Steel	Cast Alloy Steel	
	Production/Use Region	Europe	Europe	
	Shipping	Truck	Truck	
	Weight	87.41	87.41	g
	Surface Area	15737.76	15737.76	mm^2
	Transportation Distance	500	500	km
Carbon Footprint	Material	0.198	0.198	kg CO_2e
	Production	0.175	0.035	kg CO_2e
	Shipping	2.1E-3	2.1E-3	kg CO_2e
	End of Use	0.079	0.079	kg CO_2e
	Total	0.454	0.314	kg CO_2e
Total Energy Consumed	Material	2.4	2.4	Mj
	Production	3.3	0.675	Mj
	Shipping	0.030	0.030	Mj
	End of Use	0.736	0.736	Mj
	Total	6.5	3.9	Mj
Air Acidification	Material	6.0E-4	6.0E-4	kg SO_2e
	Production	9.6E-4	2.4E-4	kg SO_2e
	Shipping	9.6E-6	9.6E-6	kg SO_2e
	End of Use	3.5E-4	3.5E-4	kg SO_2e
	Total	1.9E-3	1.2E-3	kg SO_2e
Water Eutrophication	Material	1.7E-4	1.7E-4	kg PO_4e
	Production	4.0E-5	8.6E-6	kg PO_4e
	Shipping	2.2E-6	2.2E-6	kg PO_4e
	End of Use	4.7E-5	4.7E-5	kg PO_4e
	Total	2.6E-4	2.3E-4	kg PO_4e

solution. However, it is crucial to consider other factors that contribute to the overall value, such as the quality of the end product, the required timeframe for production, and any specific requirements or constraints. Making a well-informed decision necessitates a comprehensive evaluation of these factors to determine the most suitable approach.

Table 8
Comparing Costs: 3D Printing vs. Milled

	Optimum Design	Optimum Design
Process	Milled	3D Printing
Cost	86.13 USD/piece	23.12 USD/piece

Conclusion

A new complete approach involving CAD-Optimization and sustainability has been conducted successfully in this work. The results obtained from the finite element analysis showcased that when Cast Alloy Steel material was utilized, the brake disc rotor experienced minimal deformation, particularly around its center. This outcome provided strong validation for Model 1, demonstrating its reliability in real-world applications. Furthermore, the implementation of topology optimization analysis on Model 5 yielded promising results in terms of displacement, stress, and strain. These favorable outcomes further solidified the validation of Model 5 as the optimal structure for the brake system.

In addition, to performance considerations, sustainability analysis played a crucial role in the evaluation process. The results of this analysis revealed that the Milled manufacturing process exhibited a higher degree of environmental friendliness compared to the Sand Casted process. The Milled process demonstrated a reduced environmental impact by emitting lower levels of polluting gases, such as CO_2, SO_2, and PO_4. Moreover, it was observed that the Milled process consumed less energy, contributing to overall energy conservation. These findings highlight the importance of considering sustainable manufacturing practices when developing the optimal structure for the brake system.

Furthermore, the comparison of costs between the printing process and the milled process underscores a noticeable discrepancy. The printing process emerges as the more economically advantageous choice, presenting a cost advantage over the milled process, which involves higher expenses. However, it is crucial to take into account supplementary factors like product quality, production timeframe, and specific requirements to make an informed decision. Conducting a comprehensive evaluation of these aspects is pivotal in determining the optimal approach that strikes a balance between cost-effectiveness and other essential considerations. Ultimately, this approach ensures the maximization of overall value in the decision-making process.

Acknowledgments

Funding The authors declare that no funds, grants, or other support were received during the preparation of this manuscript.

References

Adeyi, A.J., Adeyi, O., Isola, B.F., Areghan, S.E., Oke, E.O., Ogunsola, A.D., & Adetunji, M.O. (2024). Sustainability of Forest Resource Utilization: A Life Cycle Assessment Study. *Sustainable Production and Consumption of forest products*, 221.

Bhat, A., Pal, B., & Dandotiya, D. (2024). Structural analysis of a two-wheeler disc brake. In *IOP Conference Series: Materials Science and Engineering*, (Vol. 1013, No. 1, p. 012024). IOP Publishing.

Cheng, Y., Liu, W., Wang, T., Li, T., & Huang, Q. (2024). Study on the effects of initial temperature and thickness ratio of component metals on the preparation of aluminum/steel clad plates by the new different temperature rolling method. *Journal of Manufacturing Processes*, 95, 229–241.

Deng, B.Y., Li, L.Z., Tan, D., Uddin, M.N., Cai, Z.W., & Yu, K.Q. (2024). Sustainable and cost-effective ultra-lightweight engineered cementitious composite: Design and material characterization. *Cement and Concrete Composites*, 136, 104895.

Elhilali, F., Fihri-Fassi, H., & Ourihi, R. (2024). Towards the development of an optimized numerical model of the brake system pad with natural material. Materials Today: Proceedings, 45, 5419–5425.

Fihri-Fassi, H., Ourihi, R., & Elahrach, K. (2024). An integrated method involving design-manufacturing-environment applied in strutural optimization. *Materials Today: Proceedings*, 38, 135–138

Fihri-Fassi, H. EcoDesign Innovation (2024). https://ecodesign.ma, https://app.ecodesign.ma.

Garg, R., Sharma, A., Singh, D., Mishra, J., & Gehlot, A. (2024, June). Braking in Electrical Vehicle for Control of heat flow. In *2024 3rd International Conference on Intelligent Technologies (CONIT)* (pp. 1–6). IEEE.

Gumiel, J. Á., Mabe, J., Burguera, F., Jiménez, J., & Barruetabeña, J. (2024). Next-generation pedal: integration of ensors in a braking pedal for a full brake-by-wire system. *Sensors*, 23(14), 6345.

Hamada, A.T., & Orhan, M.F. (2022). An overview of regenerative braking systems. Journal of Energy Storage, 52, 105033.

Huchtkoetter, P., Neubeck, J., & Wagner, A. (2024, July). Analysis of Brake-Drag in Disc Brakes on Vehicle-Level. In *International Stuttgart Symposium* (pp. 140–155). Wiesbaden: Springer Fachmedien Wiesbaden.

Isacco, L., La Mura, F., & Giberti, H. (2024). Brake System Model for a Haptic Brake Pedal Control. In *2024 5th International Congress on Human-Computer Interaction, Optimization and Robotic Applications (HORA)* (pp. 01–05). IEEE.

Kamiński, Z. (2022). Calculation of the optimal braking force distribution in three-axle trailers with tandem suspension. *Acta Mechanica et Automatica*, 16(3), 189–199.

Kien, D.N., & Zhuang, X. (2024). Radial basis function based finite element method: Formulation and applications. *Engineering Analysis with Boundary Elements*, 152, 455–472.

Kladovasilakis, N., Kosmidis, G., Kyratsis, P., & Tzetzis, D. (2024). Topology Optimization Utilizing Density-Based Approach for Additive Manufactured Components: A Case Study of an Automotive Brake Caliper. In *Computational Design and Digital Manufacturing* (pp. 91–106). Cham: Springer International Publishing.

Kumar, D., Angra, S., & Singh, S. (2022). Mechanical properties and wear behaviour of stir cast aluminum metal matrix composite: a review. *International Journal of Engineering*, 35(4), 794–801.

Kumar, N., Singh, J., & Jiwari, R. (2024). Convergence analysis of weak Galerkin finite element method for semilinear parabolic convection dominated diffusion equations on polygonal meshes. *Computers & Mathematics with Applications*, 145, 141–158.

Kumbhar, B.K., Patil, S.R., & Sawant, S.M. (2017). A comparative study on automotive brake testing standards. *Journal of The Institution of Engineers (India): Series C*, 98, 527–531.

Ma, L., Ding, S., Zhang, C., Huang, Y., & Zhang, X. (2024). Study on the wear performance of high-speed railway brake materials at low temperatures under continuous braking conditions. *Wear*, 512, 204556.

Made in China (2024). https://talfri.en.made-in-china.com/20/12/2024.

Mahfouz, A.M., Mohammed, M.H., Shams, S., & Abbas, H.S. (2024). Accurate and Simple Modeling of Eddy Current Braking Torque: Analysis and Experimental Validation. *IEEE Transactions on Magnetics*, 59(4), 1–9.

Makeshkumar, M., Anburaj, J., Kumar, M.S., & Santhosh, A.J. (2024). Effect of zirconium and niobium on the microstructure and mechanical properties of high-strength low-alloy cast steels. *Materials Research Express*, 10(5), 056506.

Meiklejohn, D.A., Khan, Z.H., Nuñez, K.M., Imhof, L., Osmani, S., Benavidez, A.C., & Tarefder, R. (2024). Environmental impact of adult tonsillectomy: life cycle assessment and cost comparison of techniques. *The Laryngoscope*, 134(2), 622–628.

Mrausi, S., Trimble, J., Olabanji, O., Tlhabadira, I., & Daniyan, I.A. (2024, May). Investigating the Mechanical Properties of Automotive Brake Disc and Pad Developed from Locally Sourced Materials. In *2024 14th International Conference on Mechanical and Intelligent Manufacturing Technologies (ICMIMT)* (pp. 197–203). IEEE.

Nguyen, N.C., Vila-Perez, J., & Peraire, J. (2024). An adaptive viscosity regularization approach for the numerical solution of conservation laws: Application to finite element methods. *arXiv preprint* arXiv:2305.00461.

Ourihi, R., Fihri-Fassi, H., & El-Hilali, F. (2024). The optimum size of pet prosthetic for additive manufacturing. *Materials Today: Proceedings*, 45, 5725–5731.

Rahmzadeh, A., Alam, M.S., & Tremblay, R. (2024). 3D response simulation of a bridge with a posttensioned base rocking steel pier under sequential loading of traffic loads, braking force, and earthquake excitations. Earthquake Engineering & Structural Dynamics.

Sahoo, S., Veerendar, C., & Prakash, S.S. (2024). Experimental and numerical studies on flexural behaviour of lightweight and sustainable precast fibre reinforced hollow core slabs. *Construction and Building Materials*, 377, 131072.

Singh, R.K., & Sarkar, C. (2024). Two-wheeler magnetorheological drum brake operating under hybrid mode for enhancing braking torque: Development and validation. Mechatronics, 92, 102971.

Talati, F., & Jalalifar, S. (2008). Investigation of heat transfer phenomena in a ventilated disk brake rotor with straight radial rounded vanes. *Journal of Applied Sciences*, 8(20), 3583–3592.

Tomozei, I., Axinte, T., & Cazacu, M. (2024). Cantilever Beam: A New Approach. *International Journal of Advanced Multidiscilinary Research and Studies*, 3(3), 448-450.

Usmani, D., Mohan, R., Mewada, C.S., & Goga, G. (2024, May). A comprehensive literature review on the recent advances in braking systems technology using FEA. In *Journal of Physics: Conference Series*, Vol. 2484, No. 1, p. 012034. IOP Publishing.

Veeman, D., Katiyar, J.K., & Ruggiero, A. (2024). Tribomechanical performance of brake composite material: a comprehensive review. *Tribology-Materials, Surfaces & Interfaces*, 1–24.

Wagh, N.P. (2005). Design and analysis of modular caliper assembly. Wichita State University.

Wang, X., Li, W., Li, Z., Li, Z., & Zhang, F. (2024). Effect of braking torque on vehicle nonlinear dynamics. *Meccanica*, 58(7), 1267–1289.

Wei, L., Wang, X., Liu, H., & Li, L. (2024). System modeling, experimental validation and pressure estimation of the pneumatic braking system. *Mechanical Systems and Signal Processing*, 187, 109938.

Yan, Q., XiaoLong, W., ChaoLiang, S., Sheng, S., Lou, W., & Shuai, G. (2022). Design of Brake Disc Dust Cover Based on Multidisciplinary Optimization Method. In *Proceedings of China SAE Congress 2024: Selected Papers* (pp. 881–891). Singapore: Springer Nature Singapore.

Yu, C., Zhang, W., Jiang, R., Wu, Y., & Xiao, H. (2024). Preparation Method and Properties of Q235/5083 Composite Plate with 1060 Interlayer by Differential Temperature Rolling with Induction Heating. *Metals*, 13(9), 1501.